IOP Publishing Journal of Optics A: Pure and Applied Optics
J. Opt. A: Pure Appl. Opt. **9** (2007) S315–S321 doi:10.1088/1464-4258/9/9/S06

Near-field driving of a optical monopole antenna

Tim H Taminiau[1], Frans B Segerink[2], Robert J Moerland[2], L (Kobus) Kuipers[3] and Niek F van Hulst[1,4,5]

[1] ICFO—Institut de Ciencies Fotoniques, Mediterranean Technology Park, 08860 Castelldefels (Barcelona), Spain
[2] Applied Optics Group, MESA+ Institute for NanoTechnology, University of Twente, 7500 AE Enschede, The Netherlands
[3] FOM Institute for Atomic and Molecular Physics (AMOLF), Kruislaan 407, 1098 SJ Amsterdam, The Netherlands
[4] ICREA—Institució Catalana de Recerca i Estudis Avançats, 08015 Barcelona, Spain

E-mail: Niek.vanHulst@ICFO.es

Received 23 May 2007, accepted for publication 4 July 2007
Published 22 August 2007
Online at stacks.iop.org/JOptA/9/S315

Abstract
Nanosized optical antennas have the potential to confine and enhance optical electromagnetic fields, making nano-antennas essential tools for applications in integrated nano-optical devices and high-resolution microscopy. The size, shape and material of the nano-antenna, together with the optical frequency, determine the antenna response and its resonances. Here, we discuss a $\lambda/4$ long optical nano-antenna, analogous to the radio frequency monopole antenna. The antenna is fabricated at the end of a near-field aperture-type fibre probe by focused-ion-beam milling in two sequential steps. Illumination through the fibre creates a localized evanescent excitation source, with the advantage of a lower background compared to 'apertureless' techniques, which require far-field excitation. Previously, we have studied the field localization, antenna excitation conditions and antenna resonances, both in experiment, by near-field single-molecule detection experiments, and in theory, by finite integration technique simulations. In this study we investigate the importance of both polarization conditions and antenna position in creating an efficient local driving field for the monopole antenna. It is shown that the antenna is driven by the field component along the antenna axis. Next we show the advantage of the antenna over the aperture: upon reduction of the diameter the antenna gains local field intensity, while the aperture field decreases rapidly. Finally, the highly localized field near the antenna apex is probed by single molecules and detected molecular emission features below 30 nm FWHM are presented.

Keywords: nano-antenna, optical antennas, monopole, plasmonics, single molecule detection, nanotechnology

1. Introduction

Antennas are usually associated with radio waves and electronic circuits. For visible light waves, at optical frequencies, one automatically thinks of lamps, lenses, lasers, fibres, etc. Though both types of wave are electromagnetic in nature, clearly the giant leap in frequency has lead to seemingly unrelated appearances in everyday use. Only recently, moving towards the nanometre scale, is the concept of optical antennas gaining interest [1]. This is mainly because the diffraction limit is a serious obstacle in the use of classical optical

[5] www.icfo.es

lenses/mirrors, and progress in nanoscale optics thus requires alternative approaches. Indeed the exploration of novel designs, using sharp tips, nanoparticles, plasmonic resonances and 'superlensing' metamaterials, is a topic of extreme interest in current optical research. Surprisingly, the vast amount of highly developed radio frequency antenna designs, which can give important clues how to proceed at optical frequencies, has hardly been exploited. In fact the connections between the nano-optical and radio wave antenna communities (optical physicists and electrical engineers, respectively) have so far been limited, which reflects the serious challenges to fabricate nano-optical antennas and the obstacles to address the induced currents and fields at optical frequencies.

Currently most nano-antenna research concerns planar structures on glass substrates: resonant metallic (often gold) dots and bars of various shape and size [2], and various metallic gap structures, e.g. dimers and bow-ties [3, 4]. The local antenna field is addressed by linear methods (scattering, luminescence and Raman) [5], nonlinear methods (two-photon luminescence, second harmonic generation) [6, 7] and near-field probing [8]. Recently electron spectroscopy in particular has proven powerful to map the local plasmonic fields on such surface nano-antennas [9].

Free-standing nano-antennas have been reported only in a few geometries. Of course the classical near-field aperture probe [10] could be considered as a (complicated) inefficient nano-antenna. However, the concept of the circular aperture originates from attempts to squash the confocal spot and from fabrication limits. In terms of antenna concepts though, a simple circular hole is far from optimum. For example, an optimized C-shaped aperture can provide up to three orders of magnitude more power throughput for a similar area [11]. The notion of hole resonances was only recently triggered by the extraordinary transmission in hole arrays [12]. In the same way, the sharp metallic (or semiconductor) 'apertureless' tips used in tip-enhanced microscopy are mainly motivated by the 'lighting rod effect' instead of plasmonic antenna resonances. Recently, gold nanoparticles attached to glass tips have been exploited as nano-antennas by both the Novotny and Sandoghdar groups [13–15]. In these elegant experiments field enhancement, radiative decay modification, quenching and even strong four-wave mixing [16] were reported. Simultaneously the Hecht, Kino and Capasso groups are experimenting with bowtie-shaped antenna probes [6, 17, 18].

Recently we presented the first optical monopole antenna probe [19, 20]. In scaling down the basic radio-wave monopole, the finite conductivity at optical frequency requires a serious redesign of the antenna. In particular, the length of the antennas needs to be carefully adjusted to obtain resonance. Moreover, one needs to reconsider how to drive such a monopole. We decided to drive the nano-optical monopole antenna by the near-field of a conventional sub-wavelength aperture probe, yielding the advantage of background-free excitation. The local antenna field was probed exploiting single fluorescent molecules as point detectors. The molecules appeared as fluorescence features smaller than 30 nm, i.e. super-resolution of $1/20$ of the optical wavelength (514 nm), reflecting the field confinement at the antenna apex. The highest field enhancement was observed for antennas of 70–90 nm length, in good agreement with the effective $\lambda/4$ length of an aluminium monopole with 20 nm radius at 514 nm wavelength [19].

Here we focus on the $\lambda/4$ long (resonant) monopole antenna and put it in the context of common nanoscale optical probes. We study the feeding of the antenna through a sub-wavelength aperture by finite integration technique calculations of the local electromagnetic field for an aperture and for the aperture–monopole configuration. It is shown that only the local field component oriented along the antenna axis couples to the antenna, in good agreement with previous experimental results. The fundamental advantage of the aperture-fed monopole over the standard aperture probe is demonstrated by calculations for different aperture and antenna radii. Finally, we demonstrate how creative three-dimensional (3D) milling with focused-ion-beam technology can be used to fabricate free-standing metallic antennas of controlled length arbitrarily placed on the end face of standard aperture probes.

2. Apertures, scattering tips and antennas

Experiments on nanoscale optical probes date back to the work on sub-wavelength apertures by Pohl and co-workers [21] at IBM Zurich in the early 1980s. Simultaneously, Wessel proposed a complementary approach based on a resonant nanoparticle [22]. To date both schemes are still the basis for the dominant approaches in near-field scanning optical microscopy (NSOM). As sketched in figure 1, the conventional NSOM is based on an aperture at the end of a glass fibre, while the scattering tip (or 'apertureless') type NSOM is a sharp metallic tip, at which the field is locally enhanced. Each method has its specific advantages and disadvantages. For 'aperture' NSOM (figure 1(a)), throughput is a limiting factor; smaller apertures give a large reduction in output power density, limiting the workable aperture size to a minimum of about 70 nm [10, 23–25]. For 'apertureless' NSOM (figure 1(b)) the resolution can reach 10 nm; however, the diffraction-limited illumination creates a problem [26–31] in discriminating the signal from neighbouring background contributions. This requires modulation techniques to extract the near-field signal contribution [32, 33]. Despite more than two decades of development, the widespread application of NSOM is still hindered by the absence of a robust and versatile probe that combines high throughput (beyond cut-off), zero background and optical field confinement within a few nanometres.

Frey *et al* [34] presented the 'tip-on-aperture' (TOA) by placing a metallic tip on top of a normal nano-aperture, a method that combines the best of both worlds. It exploits the high resolution from apertureless NSOM with the background-free aperture design, as sketched in figure 1(c). Indeed, Frey *et al* [35] showed single-molecule detection, with details as small as 10 nm, free of far-field background. However, the tip was considered more as a scattering tip than as an antenna, and resonances and excitation conditions were not considered. Here we deal with such a tip excited at resonance, i.e. a monopole antenna, and focus particularly on the antenna driving conditions.

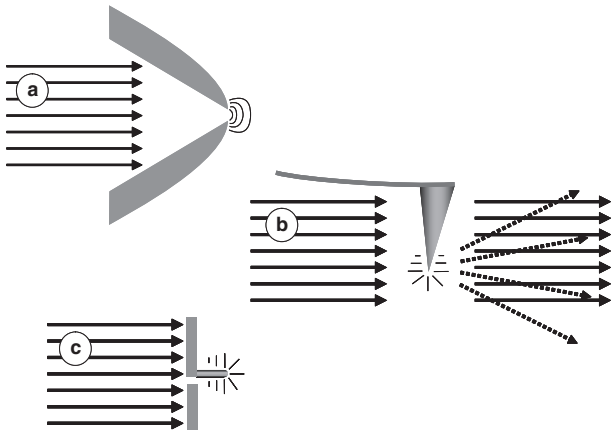

Figure 1. Several near-field probe arrangements. The aperture probe (a) generates background-free local fields, however with low throughput. The tip-enhanced approach (b) generates efficiently strong local fields, however with appreciable far-field background. The alternative (c) of a resonant antenna driven by the aperture near field efficiently generates local fields free of background.

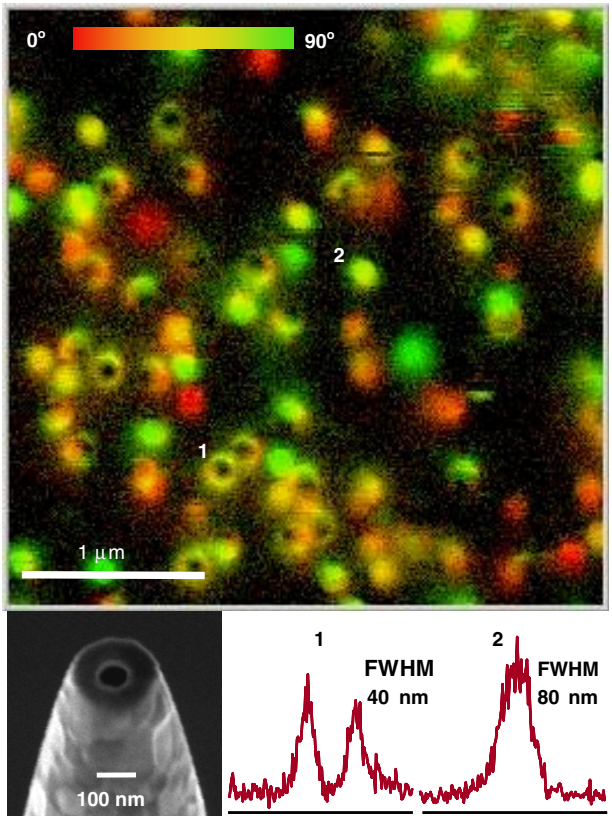

Figure 2. Near-field image showing the spatial fluorescence profile of several single molecules (DiI in PMMA) excited by an aperture probe. The signal is colour-coded according to the polarization of the fluorescence (red horizontal, green vertical). The inset shows a 75 nm aperture probe fabricated by FIB milling and typical fluorescence line traces for selected molecules oriented out of plane (1) and in plane (2).

3. Antenna fed by aperture probe

A monopole antenna is fed at its base with a localized field orientated along the antenna axis. Like in the TOA configuration, a sub-wavelength aperture can fulfil this role. The sharp dielectric-metal rim provides a well-defined highly localized evanescent field, as shown experimentally in detail by several groups in the past [10, 36, 37]. High-definition apertures are routinely fabricated on metal-coated tapered optical fibres by a final focused-ion-beam (FIB) polishing process [23]. With 75–100 nm apertures and brightness up to $\sim$1 μW, these classical NSOM probes are sufficient for high-resolution single-molecule detection. Figure 2 shows such a high-resolution map of single fluorescent molecules excited by an aperture probe with a flat end face. The excitation polarization is circular and the collected fluorescence of the molecules is detected in both polarization directions, represented by the green and red pseudo-colours. A variety of characteristic near-field patterns can be observed [36]. In particular, molecules oriented perpendicular to the probe facet show up as ring or lobe patterns in the fluorescence image (e.g. molecule 1 in figure 2). This reflects the strong evanescent optical field component, oriented out of plane, at the sharp glass–aluminium transition at the rim of the aperture. Intuitively, for a monopole antenna on the ground plane of the aperture probe, the rim seems a good position. The local aperture field provides the right evanescent field component, located at the antenna base and orientated along the antenna axis, needed to efficiently drive the antenna.

In practice the optical field distribution around the aperture–monopole system can be rather complex. To this end we have simulated 3D electric field distributions using the finite integration technique (FIT) [38]. Figure 3 presents FIT calculations showing the averaged field intensity for the case of an aperture, with and without the monopole antenna. The aperture is placed in a 10 nm thick, perfectly electrically conducting (PEC), metal screen. For incident linearly polarized light, the out-of-plane (z) field component is concentrated in two lobes on the aperture edge in the direction of the incident polarization. Note that, if a monopole antenna is present, this field component is orientated along the antenna axis. The position of the lobes rotates with the incident polarization (x- or y-direction in figure 3(a)). Next, the monopole antenna, PEC and 100 nm long with a 20 nm radius, is positioned close to the edge in the y-direction, as sketched in figure 3(b). For incident y-polarized light the antenna is fed efficiently, resulting in strong total field intensity at the antenna apex. The field is enhanced compared to the field in the aperture without antenna. For incident x-polarized light the antenna is not excited, and only the much weaker field of the distant aperture remains. Only the local field orientated along the antenna axis efficiently couples to the antenna.

To further strengthen this notion, the influence of the exact position of the monopole antenna is investigated. In figure 4, calculated field intensity maps are plotted for an antenna at different locations. When, for example, the antenna is placed in the middle of the aperture (figure 4(a)) the local field is, although strong, not orientated along the antenna axis, and the antenna is not fed. The strongest antenna field is found when the antenna axis coincides with the aperture edge (figure 4(b)). An antenna further away from the aperture is also driven, yet less efficiently (figure 4(c)). In figure 4(d) the field intensity

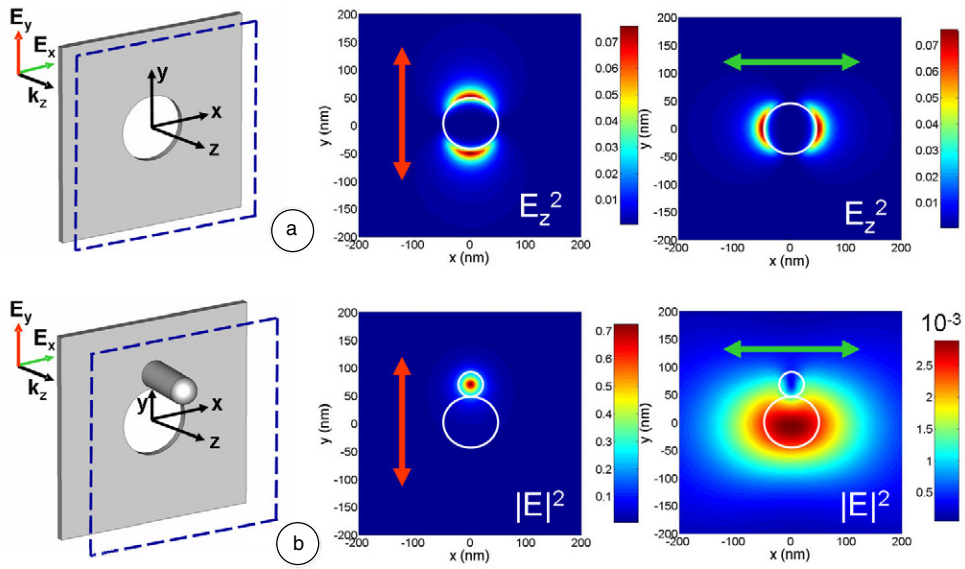

Figure 3. FIT calculations of the local field intensity for a ⌀ 100 nm aperture both without (a) and with (b) antenna in a plane 10 nm below the aperture (in (a)) or antenna apex (in (b)). A strong out-of-plane (z) oriented field is observed at the edge of the aperture in the direction of the incident polarization (a) [10, 36]. With the antenna (20 nm radius) positioned at the aperture edge a strong and confined (30 nm FWHM) field occurs at the antenna apex, for incident linear polarization in the direction of the antenna. For perpendicular polarization the antenna is not driven and only a weak aperture field is observed.

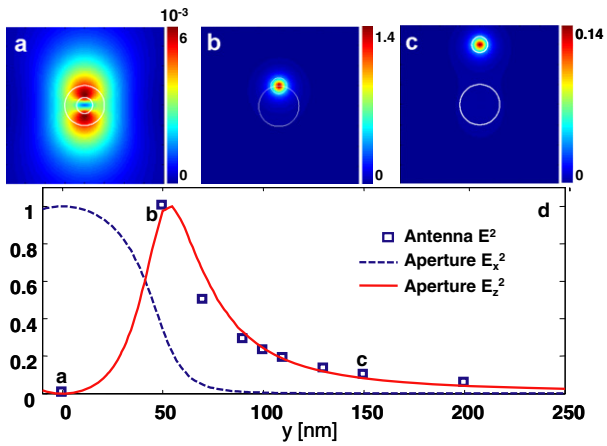

Figure 4. The effect of antenna position for incident polarization in the antenna direction (y). (a) Field intensity for a monopole positioned at the centre of the aperture. (b) Field intensity for a monopole with its axis on the aperture edge. (c) Field intensity for a monopole positioned 100 nm from the aperture edge. (d) Intensity of the antenna apex field and the bare aperture x- and z-field components, as a function of the position (y) from the aperture centre, with positions of (a), (b) and (c) indicated.

at the antenna apex is plotted as a function of the antenna position, together with the in-plane (x) and out-of-plane (z) field intensity of the flat aperture (without any antenna). The monopole field follows perfectly the decay of the z-field for increasing distance away from the aperture, proving that the monopole is indeed driven by the aperture z-field. Remarkably, one can thus predict the response of the monopole by looking at the local field of a simple aperture, even though the field is clearly modified after placing the antenna.

It is interesting to examine the effect of reducing aperture size or antenna radius on the local field intensity and confinement. To get accurate results for various antenna radii, it is important to use the correct optical material properties. Here we use $\varepsilon = -31.3 + 8.0\mathrm{i}$ as the dielectric constant for aluminium at 514 nm. In figure 5 a typical case is plotted. When reducing the aperture size with a factor of two (radius from 100 to 50 nm), the highest field intensity at 20 nm distance from the aperture reduces by a factor ∼30. When reducing the antenna radius (from 30 to 15 nm), the highest field intensity increases about five times, i.e. an enhanced power density. The calculated trends upon size reduction nicely illustrate the advantage of antenna-enhanced field confinement. In the case of the aperture there is a trade-off between confinement and intensity, while for a sharper antenna both the confinement and intensity improve. Of course the antenna field enhancement has its limits; absorption losses will start dominating for very thin non-perfectly conducting antennas.

4. Local antenna field probed by single molecules

The antenna probes are fabricated by building on the established fabrication of aperture probes, using a dual-beam (FIB and electron microscopy) machine [23]. We carve the antennas directly by FIB sculpting, with the aluminium-coated pulled fibre acting as a platform. The metal is removed in several milling steps (see figure 6) until the uncovered aperture and antenna have the desired dimensions. With this precise and flexible method, we have fabricated several types of monopole nano-antenna with varying position and length of the antenna, to tune the monopole to resonance, as well as varying the aperture size.

To measure the extent of the local field at the monopole apex we again exploit single fluorescent molecules as local point detectors. To this end the antenna probe is mounted in a near-field optical microscope set-up, with a ‘single-molecule’

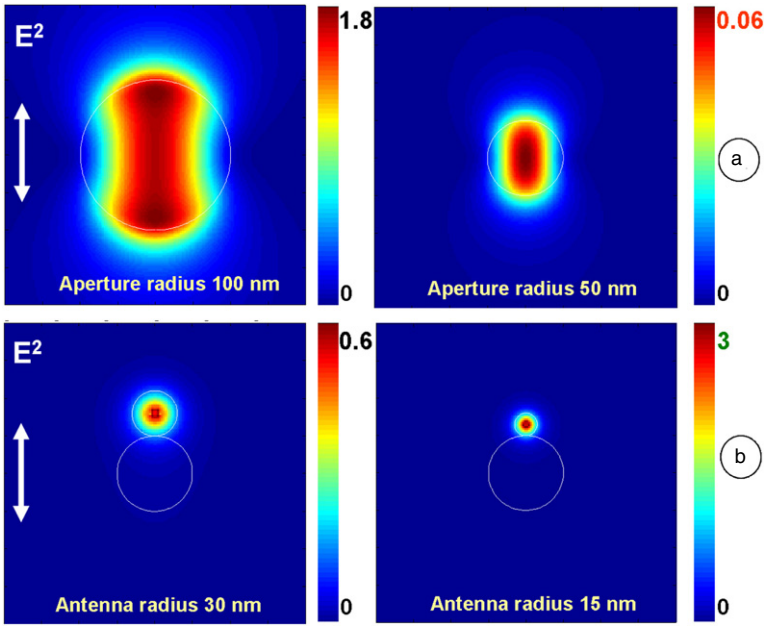

Figure 5. The effect of reducing sizes. (a) FIT calculations of the field intensity in a plane 20 nm below the aperture; and (b) FIT calculations of the field intensity in a plane 5 nm below the antenna. The field at the heart of the aperture decreases rapidly by reducing the aperture radius from 100 to 50 nm. The field at the antenna increases upon reducing the antenna radius from 30 to 15 nm.

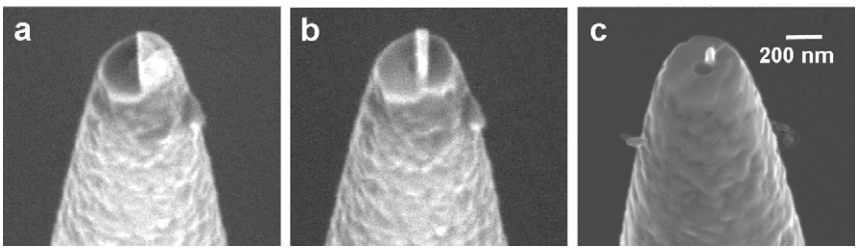

Figure 6. Fabrication process of antenna probes by FIB milling. In several steps, the antenna is carved out of an aluminium-coated pulled fibre probe. First, sections on both sides are removed, such that a narrow ridge is created ((a), (b)). Next, the probe is rotated and the final antenna is shaped by thinning down the ridge. The length of the antenna is trimmed with 5 nm accuracy, up to over 100 nm, to tune the antenna resonances.

sample of DiI molecules embedded in PMMA. Green light (514 nm wavelength) is coupled into the fibre to drive the monopole and excite the DiI fluorescence. The fluorescence of the molecules is collected with a high numerical aperture (NA 1.3) objective, and the two orthogonal polarization directions are detected with two avalanche photodiodes (APDs). The sample is scanned and the antenna kept at ∼10 nm distance from the PMMA surface by tuning fork based shear force sensing. Figure 7 shows some images of fluorescent single DiI molecules using the antenna probe for excitation. The images show two distinct features. In figure 7(a) one recognizes both small sharp fluorescent spots (∼30 nm) and larger spots (∼150 nm). The larger spots show green–yellow–red polarization pseudo-colour, indicating mainly in-plane oriented molecules with different emission dipole moment, excited by the remnant aperture field. The sharp spots are associated to monopole antenna excitation and show more isotropic polarization emission character. Between figures 7(a) and (b) the incident polarization was rotated over 90°. Clearly, in figure 7(b) all sharp spots have disappeared, leaving only larger aperture related spots. On rotating the polarization back, the small spots are again retrieved. This behaviour was observed for all antenna probes fabricated and clearly shows the importance to feed the antenna with the right input polarization, as sketched in figures 7(c) and (e) and predicted by the FIT simulations in figure 3. The inset (figure 7(d)) with a fluorescence profile of a selected single molecule displays a half width of ∼30 nm, which is indicative of the field localization at the antenna apex and in agreement with the field simulations for a 20 nm radius aluminium antenna.

5. Conclusions

We have presented a nano-optical monopole antenna, in direct analogy with the conventional radio-frequency case. The monopole antenna is driven by the local field of a sub-wavelength aperture. Calculations of the local field, for a simple aperture and for the monopole antenna, show that only the local field component orientated along the antenna axis couples efficiently to the antenna. In practice, this means

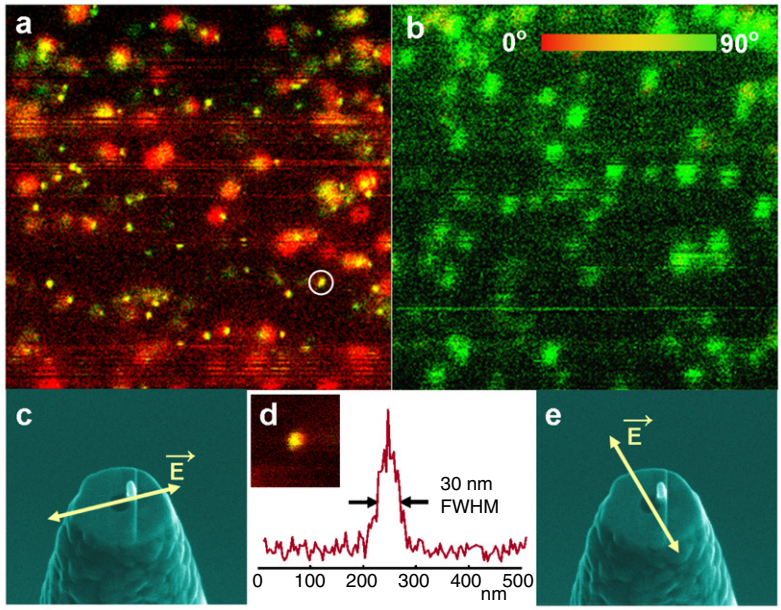

Figure 7. ((a), (b)) Single fluorescent DiI molecules excited by the antenna probe, for two directions of incident linear polarization. Two features appear: sharp spots (∼30 nm) showing molecules excited by the local monopole antenna and large spots (∼150 nm) associated with molecules excited by the aperture. The sharp spots only occur in (a) for the polarization that drives the antenna. ((c), (e)) Excitation polarization with respect to the position of the antenna. (d) Fluorescence line trace for a selected molecule excited by the monopole, demonstrating the localized antenna field with 30 nm FWHM at the position of the molecule.

that it is important to use the proper polarization to drive the antenna. Direct measurements of the local antenna field with single fluorescent molecules support this theory. Upon further confinement of the optical field, the antenna has a clear advantage over the aperture. For a sharper antenna both intensity and confinement improve, whereas for a smaller aperture the intensity decreases dramatically. Ultimately the antenna field confinement is limited by the finite conductivity of the metal used to fabricate the antenna.

Altogether the advantages of the monopole are obvious: high-resolution optical response with low background; single molecule sensitivity including information on the molecular orientation and position; and simultaneous collection of force-based topographical information [19].

Finally, our optical monopole antenna demonstrates how old concepts can lead to innovative tools, and hopefully open new routes to exploit more sophisticated radio antenna designs for nanoscale optical microscopy, optimized sensing and emission, lithography, data storage, etc [39].

Acknowledgments

This work is supported by ASPRINT, the Specific Target Research Project on Advanced Scanning Probes for Innovative Nanoscience & Technology (NMP-CT-2003-001601) and by the NEST-Adventure program Bio-Light-Touch, both in the 6th Framework Program of the European Community.

R J Moerland is financed by FOM, the Dutch Foundation for Fundamental Research of Matter, which is financed by NWO, the Dutch organization for academic research.

Niek van Hulst thanks Claire Bedrock of IOP Publishing for her assistance in enabling this special issue covering the 1st NanoMeta conference.

References

[1] Pohl D W 1999 Near field optics seen as an antenna problem *Proc. Near-Field Optics: Principles and Applications, Second Asia-Pacific Workshop on Near-Field Optics (Beijing, October 1999)*
[2] Rechberger W, Hohenau A, Leitner A, Krenn J R, Lamprecht B and Aussenegg F R 2003 *Opt. Commun.* **220** 137
[3] Mühlschlegel P, Eisler H-J, Martin O J F, Hecht B and Pohl D W 2005 *Science* **308** 1607
[4] Fromm D P, Sundaramurthy A, Schuck J, Kino G and Moerner W E 2004 *Nano Lett.* **4** 957
[5] Laurent G, Félidj N, Lau Truong S, Aubard J, Lévi G, Krenn J R, Hohenau A, Leitner A and Aussenegg F R 2005 *Nano Lett.* **5** 253–8
[6] Schuck P J, Fromm D P, Sundaramurthy A, Kino G S and Moerner W E 2005 *Phys. Rev. Lett.* **94** 017402
[7] ten Bloemendal D, Ghenuche P, Quidant R, Cormack I G, Loza-Alvarez P and Badenes G 2006 *Plasmonics* **1** 41
[8] Imura K, Nagahara T and Okamoto H 2005 *J. Chem. Phys.* **122** 154701
[9] Nelayah J, Kociak M, Stéphan O, García de Abajo F J, Tencé M, Henrard L, Taverna D, Pastoriza-Santos I, Liz-Marzán L M and Colliex C 2007 *Nat. Phys.* **3** 348
[10] Betzig E and Chichester R J 1993 *Science* **262** 1422
[11] Matteo J A, Fromm D P, Yuen Y, Schuck P J, Moerner W E and Hesselink L 2004 *Appl. Phys. Lett.* **85** 648
[12] Lezec H J *et al* 2002 *Science* **297** 820
[13] Kalkbrenner T, Håkanson U, Schädle A, Burger S, Henkel C and Sandoghdar V 2005 *Phys. Rev. Lett.* **95** 200801
[14] Anger P, Bharadwaj P and Novotny L 2006 *Phys. Rev. Lett.* **96** 113002
[15] Kühn S, Håkanson U, Rogobete L and Sandoghdar V 2006 *Phys. Rev. Lett.* **97** 017402
[16] Danckwerts M and Novotny L 2007 *Phys. Rev. Lett.* **98** 026104
[17] Farahni J N, Pohl D W, Eisler H-J and Hecht B 2005 *Phys. Rev. Lett.* **95** 017402

[18] Cubukcu E, Kort E A, Crozier K B and Capasso F 2006 *Appl. Phys. Lett.* **89** 093120
[19] Taminiau T H, Moerland R J, Segerink F B, Kuipers L and van Hulst N F 2007 *Nano Lett.* **7** 28
[20] Gevaux D 2007 *Nat. Photon.* **1** 90
[21] Durig U, Pohl D W and Rohner F 1986 *J. Appl. Phys.* **59** 3318–27
[22] Wessel J 1985 *J. Opt. Soc. Am.* B **2** 1538–41
[23] Veerman J A, Otter A M, Kuipers L and van Hulst N F 1998 *Appl. Phys. Lett.* **72** 3115
[24] van Hulst N F, Veerman J A, Garcia-Parajo M F and Kuipers L 2000 *J. Chem. Phys.* **112** 7799
[25] Eckert R, Freyland J M, Gersen H, Heinzelmann H, Schurmann G, Noell W, Staufer U and de Rooij N F 2000 *Appl. Phys. Lett.* **77** 3695
[26] Kawata S and Inouye Y 1995 *Ultramicroscopy* **57** 313
[27] Hillenbrand R and Keilmann F 2002 *Appl. Phys. Lett.* **80** 25
[28] Hamann H F, Gallagher A and Nesbitt D J 2000 *Appl. Phys. Lett.* **76** 1953
[29] Kramer A, Trabesinger W, Hecht B and Wild U P 2002 *Appl. Phys. Lett.* **80** 1652
[30] Sanchez E J, Novotny L and Xie X S 1999 *Phys. Rev. Lett.* **82** 4014
[31] Hartschuh A, Sanchez E J, Xie X S and Novotny L 2003 *Phys. Rev. Lett.* **90** 095503
[32] Gerton J M, Wade L A, Lessard G A, Ma Z and Quake S R 2004 *Phys. Rev. Lett.* **93** 180801
[33] Ma Z, Gerton J M, Wade L A and Quake S R 2006 *Phys. Rev. Lett.* **97** 260801
[34] Frey H G, Keilmann F, Kriele A and Guckenberger R 2002 *Appl. Phys. Lett.* **81** 5030
[35] Frey H G, Witt S, Felderer K and Guckenberger R 2004 *Phys. Rev. Lett.* **93** 200801
[36] Veerman J A, Garcia-Parajo M F, Kuipers L and van Hulst N F 1999 *J. Microsc.* **194** 477
[37] Moerland R J, van Hulst N F, Gersen H and Kuipers L 2005 *Opt. Express* **13** 1604
[38] CST Microwave Studio 5.1, www.cst.com
[39] Taminiau T H, Segerink F B and van Hulst N F 2007 *IEEE Trans. Antennas Propag.* (special issue on Optical and TeraHertz Technology) at press